

## PHASE EQUILIBRIA OF THE $\text{Bi}_4\text{Se}_3\text{-Bi}_4\text{Te}_3$ SYSTEM AND CRYSTALLOGRAPHIC STUDY OF $\text{Bi}_4\text{Se}_{3-x}\text{Te}_x$ SOLID SOLUTIONS

Gunel Zeynalova\*

Ganja State University, Ganja, Azerbaijan

**Abstract.** The phase relations in the  $\text{Bi}_4\text{Se}_3\text{-Bi}_4\text{Te}_3$  system were investigated using the results of DTA and PXRD of balanced alloys. Analysis of the experimental data showed that below the solidus, the system is stable and forms a continuous series of solid solutions with a trigonal structure. The lattice parameters of solid solutions determined from powder diffractograms by the Rietveld method increase linearly with increasing Te concentration which is in accordance with Vegard's rule.

**Keywords:** bismuth tellurides, bismuth selenides, tetradymite-type structure, phase equilibria, solid solutions, topological insulators.

**Corresponding Author:** Gunel Zeynalova, Ganja State University, Ganja, Azerbaijan,  
e-mail: [gzeynalova1989@gmail.com](mailto:gzeynalova1989@gmail.com)

**Received:** 18 June 2021;

**Accepted:** 28 July 2021;

**Published:** 07 August 2021.

### 1. Introduction

Tetradymite-type layered bismuth chalcogenides have long been in the center of close attention of researchers as advanced functional materials. These compounds, especially  $\text{Bi}_2\text{Se}_3$  and  $\text{Bi}_2\text{Te}_3$ , as well as solid solutions, doped phases, and composites based on them, are intensively studied as thermoelectric materials and are used in the manufacture of portable refrigerators, temperature control devices, and for power generation at space stations, etc (Rowe, 2006; Shevelkov, 2008, Tumelero *et al.*, 2019; Duong *et al.*, 2017; Witting *et al.*, 2020; Goldsmid, 2014). After the discovery of a new quantum state of matter - a topological insulator (TI) (Moore, 2010; Hasan *et al.*, 2010; Kane *et al.*, 2011), it was shown that these phases also exhibit the properties of TI, and are extremely favorable for various applications, including spintronics, quantum computers, medicine, security systems, etc (Sultana *et al.*, 2017; Le *et al.*, 2017; Pesin *et al.*, 2012; Politano *et al.*, 2015; Heremans *et al.*, 2017, Hogan *et al.*, 2019).

However, an analysis of literature data shows that in contrast to  $\text{Bi}_2\text{Te}_3$ , the functional properties of the mixed-layer compounds of the  $n\text{Bi}_2\cdot m\text{Bi}_2\text{Te}_3$  homologous series have been studied very poorly, which is apparently due to the difficulty of obtaining high-quality samples, particularly monocrystals.

The development of methods and optimization of the conditions for the synthesis of compounds and the design of materials, especially in the so-called alloy systems, requires knowledge of phase equilibria and reliable thermodynamic data of the corresponding systems (Babanly *et al.*, 2017, 2019). At same time, systems containing compounds-structural analogs are of particular interest, since one can expect vast regions of solid solutions in them (Orujlu, 2020; Imamaliyeva *et al.*, 2020).

In this work, we present an experimental investigation of phase equilibria in the  $\text{Bi}_4\text{Se}_3\text{-Bi}_4\text{Te}_3$  system and crystallographic study of  $\text{Bi}_4\text{Se}_{3-x}\text{Te}_x$  solid solution. These

type of solid solutions by selective replacing of atoms on the same sites creates a chance to control tunable properties by adjusting the concentration of substitutional atoms.

According to (Hasanova *et al.*, 2021a), in Bi-Te binary system, a total of seven tetradymite-type layered compounds are formed according to the newly refined version of the phase diagram constructed by us.  $\text{Bi}_4\text{Te}_3$  compound melts with peritectic reaction at  $435^\circ\text{C}$  and crystallizes in rhombohedral structure (Sp.gr. $R-3m$ ) with following lattice parameters:  $a=4.4440$  and  $c=41.890$  Å (Bos *et al.*, 2007). Similarly, the Bi-Se binary system contains seven tetradymite-type layered compounds with almost stoichiometric compositions (Hasanova *et al.*, 2021b).  $\text{Bi}_4\text{Se}_3$  melts peritectically at  $556^\circ\text{C}$ . It has the same rhombohedral structure (Sp.Gr. $R-3m$ ) as  $\text{Bi}_4\text{Te}_3$  with lattice parameters of  $a=4.332$  and  $c=40.610$  Å (Okamoto 1994).

## 2. Experimental part

The alloys of the studied system were synthesized by fusing of high purity elemental bismuth, selenium, and tellurium in evacuated ( $\sim 10^{-2}$  Pa) quartz ampoules. When developing the synthesis methodology of samples, we assumed that the bulk samples of layered phases obtained by the widely used fusion method do not reach an equilibrium state even after a long period (2000–3000 h) of thermal annealing (Abrikosov *et al.*, 1960; Sher *et al.*, 1986). This is apparently because, unlike conventional bulk samples, van der Waals phases obtained in non-equilibrium crystallization conditions (i.e., ordinary cooling of the melt) practically do not undergo any changes during further thermal treatment due to very low diffusion between layers.

Taking this into account, to ensure a high dispersion of samples, after alloying, samples were quenched by dropping ampoules into the ice water from a liquid state ( $600^\circ\text{C}$ ). Additionally, all samples were annealed at temperatures of  $400\text{--}500^\circ\text{C}$  depending on the compositions to obtain equilibrium compositions.

Studies were carried out by powder X-ray diffraction (PXRD) and differential thermal analysis (DTA) techniques. DTA curves were recorded on a NETZSCH 404 F1 Pegasus system. Powder diffractograms of the initial compounds and intermediate alloys were recorded using Bruker D2 diffractometer with  $\text{CuK}\alpha_1$  radiation in the range of  $2\theta = 5\text{--}75^\circ$ . The indexing of the PXRD patterns and the refinement of the lattice parameters were implemented using the FullProf software by the Le Bail method.

## 3. Results and discussion

The PXRD patterns of equilibrated alloys are shown in Fig. 1a. As can be seen, each intermediate alloy has qualitatively identical diffractograms with primary binary compounds. An analysis of these diffraction lines shows that they are fully indexed in rhombohedral structure with space group  $R-3m$ . The lattice parameters of all alloys were determined by the Rietveld technique. The observed and calculated data of the powder diffraction pattern belongs to alloy with 60 mol%  $\text{Bi}_4\text{Te}_3$  composition are shown in Fig. 1b, and determined lattice parameters of alloys are given in Table. As the composition changes from selenides to tellurides, the diffraction peaks undergo a slight shift in the direction of the small angles, while their total number remains unchanged. It is happened due to an increase in the lattice parameters as the tellurium concentration increases with the  $\text{Se}\rightarrow\text{Te}$  substitution. It was observed that lattice parameters increase linearly with increasing concentration of Te content according to Vegard's law (Fig.

2a). These results provide strong evidence that a continuous series of solid solutions are formed in  $\text{Bi}_4\text{Se}_3\text{-Bi}_4\text{Te}_3$  section.

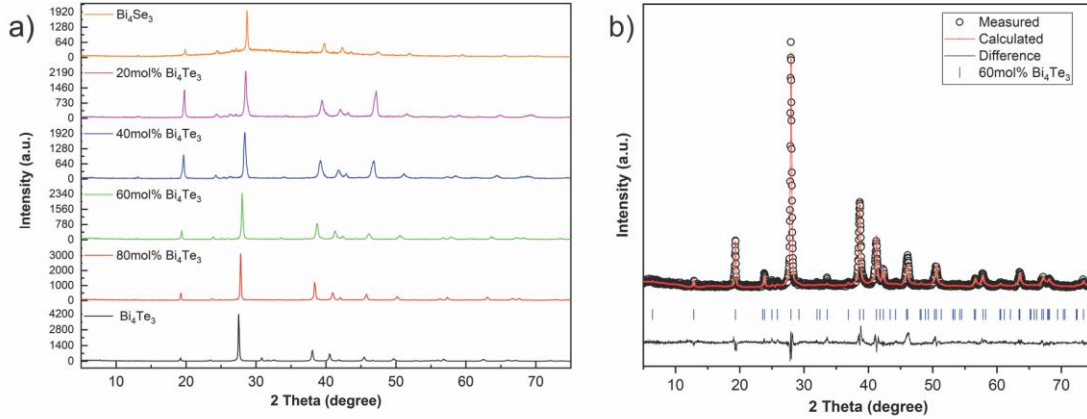


**Fig. 1.** PXRD patterns of  $\text{Bi}_4\text{Se}_{3-x}\text{Te}_x$  alloys (a) and Rietveld refinement profile of alloy with 60 mol%  $\text{Bi}_4\text{Te}_3$  composition (b)

**Table 1.** Calculated lattice parameters of  $\text{Bi}_4\text{Se}_{3-x}\text{Te}_x$  alloys

Alloys	Lattice parameters (Å)	
	<i>a</i>	<i>b</i>
$\text{Bi}_4\text{Te}_3$	4.4819	41.618
80mol% $\text{Bi}_4\text{Se}_3$	4.4381	41.386
60mol% $\text{Bi}_4\text{Se}_3$	4.3993	41.078
40mol% $\text{Bi}_4\text{Se}_3$	4.3512	40.734
20mol% $\text{Bi}_4\text{Se}_3$	4.3235	40.517
$\text{Bi}_4\text{Se}_3$	4.2786	40.211

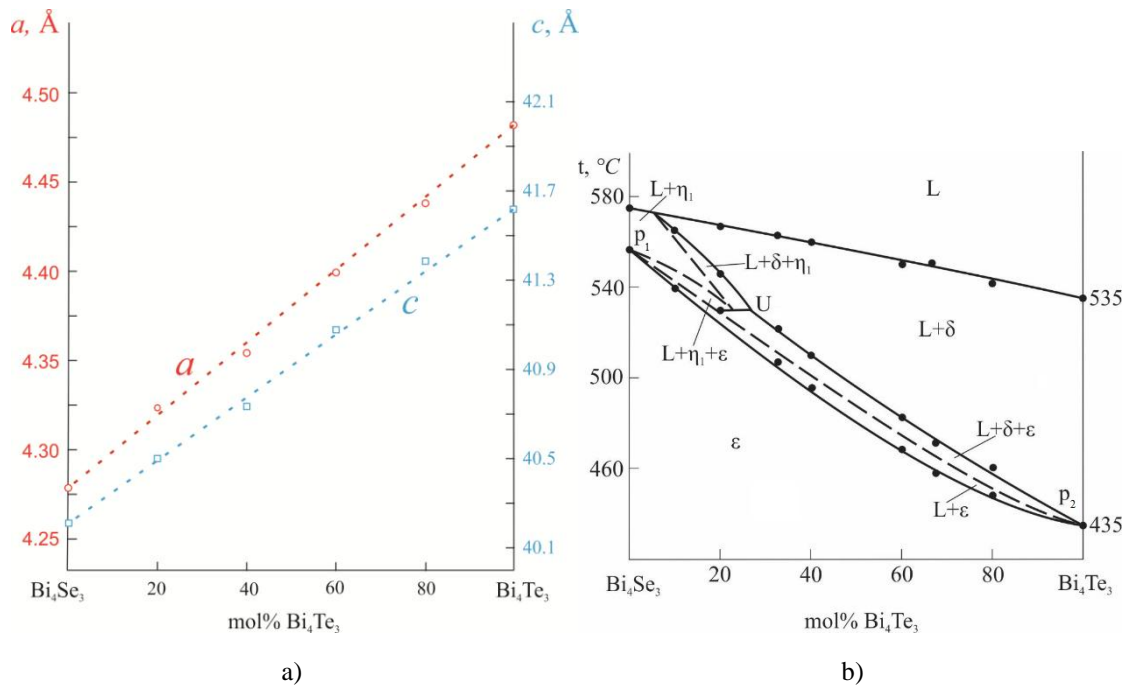


**Fig 2.** Concentration dependence of lattice parameters of  $\text{Bi}_4\text{Se}_{3-x}\text{Te}_x$  alloys(a) and phase diagram of  $\text{Bi}_4\text{Se}_3\text{-Bi}_4\text{Te}_3$  system (b)

On the basis of results obtained from DTA and PXRD examination of equilibrated alloys, as well as using liquidus projection data of the  $\text{Bi}_2\text{-Bi}_2\text{Se}_3\text{-Bi}_2\text{Te}_3$  system (Zeynalova *et al.*, 2021), a phase diagram of the  $\text{Bi}_4\text{Se}_3\text{-Bi}_4\text{Te}_3$  system were constructed, as presented in Figure 2b.

As can be seen from the constructed diagram, the system is stable below subsolidus and forms continuous solid solutions ( $\epsilon$ -phase).

Comparison the Fig.2b with the liquidus surface of the  $\text{Bi}_2\text{-Bi}_2\text{Se}_3\text{-Bi}_2\text{Te}_3$  system (Zeynalova *et al.*, 2021), shows that initially,  $\eta_1$ - phase based on  $\text{Bi}_8\text{Te}_7$  compound crystallizes from the liquid phase, while  $\delta$ -phase crystallize in 5-100 mol%  $\text{Bi}_4\text{Te}_3$  concentration range. In  $\text{Bi}_4\text{Se}_3$  rich side (0-25 mol%  $\text{Bi}_4\text{Te}_3$ ) of the phase diagram, below the liquidus line, the crystallization goes by  $\text{L}+\delta\leftrightarrow\eta_1$  and  $\text{L}+\eta_1\leftrightarrow\epsilon$  monovariant peritectic, and  $\text{L}+\eta_1\leftrightarrow\delta+\epsilon$  (U) nonvariant transition reactions. As a result,  $\text{L}+\delta+\eta_1$ ,  $\text{L}+\eta_1$ ,  $\text{L}+\eta_1+\epsilon$ , and  $\text{L}+\delta+\epsilon$  phase regions are formed in the phase diagram. The latter field is formed by the  $\text{L}+\delta\leftrightarrow\epsilon$  peritectic reaction on the  $\text{UP}_2$  curve in the 25-100 mol%  $\text{Bi}_4\text{Te}_3$  concentration range. The crystallization process finishes in the entire section by  $\text{L}\leftrightarrow\epsilon$  bivariant scheme, and a single-phase region based on  $\epsilon$ -solid solutions appears at low temperatures.

It is worth noting that according to constructed phase diagram, both phases entering the reaction with  $\text{L}+\eta_1\leftrightarrow\epsilon$  peritectic reaction must be completely consumed and monophasic  $\epsilon$ -phase must be obtained in the subsolidus area since the composition is on the corresponding quasi-stable section. However, in this case, the three-phase region along the solidus curve should contact the single-phase region, which would give the impression of a violation of the Gibbs phase rule. Therefore, in phase diagrams,  $\text{L}+\epsilon$  two-phase region are shown with a dashed line just above the solidus.

#### 4. Conclusion

In the present paper,  $\text{Bi}_4\text{Se}_3\text{-Bi}_4\text{Te}_3$  section of the Bi-Se-Te system was experimentally investigated using DTA and PXRD techniques. Based on obtained results, the phase diagram of the studied system was constructed. It was established that the system is stable below subsolidus and forms a continuous series of solid solutions in the system. The lattice parameters of solid solutions were determined using the FullProf software by the Le Bail method. Both  $a$  and  $c$  lattice parameters increase linearly with increasing concentration of Te content according to Vegard's law.

#### References

- Abrikosov, N.Kh., Bankina. V.F., Kharitonovich. K.F. (1960). Phase Diagram of the Bi-Se System. *Russ J Inorg Chem.*, 5, 978-982.
- Babanly, M.B., Chulkov, E.V., Aliev, Z.S., Shevelkov, A.V., Amiraslanov, I.R. (2017). Phase diagrams in materials science of topological insulators based on metal chalcogenides. *Russ. J. Inorg. Chem.*, 62(13), 1703-1729.
- Babanly, M.B., Mashadiyeva, L.F., Babanly, D.M., Imamaliyeva, S.Z., Taghiyev, D.B., Yusibov, Y.A. (2019). Some issues of complex investigation of the phase equilibria and thermodynamic properties of the ternary chalcogenide systems by the EMF method. *Russ.J.Inorg.Chem.*, 64(13), 1649-1671.
- Bos, J.W.G., Zandbergen, H.W., Lee, M.-H., Ong, N.P., Cava, R.J. (2007). Structures and thermoelectric properties of the infinitely adaptive series  $(\text{Bi}_2)_m(\text{Bi}_2\text{Te}_3)_n$ . *Phys. Rev. B*, 75(19), 195203.
- Duong, D.L., Yun, S.J., Lee, Y.H. (2017). van der Waals Layered Materials: Opportunities and Challenges. *ACS Nano*, 11, 11803–11830.

- Goldsmid, H.J. (2014). Bismuth Telluride and Its Alloys as Materials for Thermoelectric Generation. *Materials*, 7(4), 2577-2592.
- Hasan, M.Z., Kane, C.L. (2010). Colloquium: Topological insulators. *Rev. Mod. Phys.*, 82, 3045-3067.
- Hasanova, G.S., Aghazade, A.I., Imamaliyeva, S.Z., Yusibov, Y.A., Babanly, M.B. (2021a). Refinement of the Phase Diagram of the Bi-Te System and the Thermodynamic Properties of Lower Bismuth Tellurides. *JOM*, 73, 1511-1521.
- Hasanova, G.S., Aghazade, A.I., Babanly, D.M., Imamaliyeva, S.Z., Yusibov, Y.A., Babanly, M.B. (2021b). Experimental study of the phase relations and thermodynamic properties of Bi-Se system. *J. Therm. Anal. Calorim.*, 145, (accepted).
- Heremans, J., Cava, R., Samarth, N. (2017). Tetradymites as thermoelectrics and topological insulators. *Nat. Rev. Mater.*, 2, 17049.
- Hogan, C., Holtgrewe K., Ronci, F., Colonna, S., Sanna, S., Moras, P., Sheverdyayeva, P.M., Mahatha, S., Papagno, M., Aliev, Z. S., Babanly, M.B., Chulkov, E. V., Carbone, C., Flammini, R. (2019). Temperature driven phase transition at the antimonene Bi<sub>2</sub>Se<sub>3</sub> van der Waals heterostructure, *ACS Nano*, 13(9), 10481-10489.
- Imamaliyeva, S.Z., Alakbarzade, G.I., Gasymov, V.A., Babanly, M.B. (2020). Solid-phase equilibria diagram of the Tl<sub>2</sub>Te-TlTbTe<sub>2</sub>-TlSbTe<sub>2</sub> system. *New Materials, Compounds and Applications*, 4(2), 99-107.
- Kane, C.L., Moore, J.E. (2011). Topological Insulators. *Phys. World.*, 24, 32-36.
- Le, P.H., Liu, P.T., Luo, C.W., Lin, J.Y., Wu, K.H. (2017). Thickness-dependent magnetotransport properties and terahertz response of topological insulator Bi<sub>2</sub>Te<sub>3</sub> thin films. *J. Alloy. Compd.*, 692, 972-979.
- Matsushita, T., Mukai, K. (2018). *Chemical Thermodynamics in Materials Science: From Basics to Practical Applications*. Springer, 263.
- Moore, J.E. (2010). The birth of topological insulators. *Nature*, 464, 194-198.
- Okamoto, H. (1994). The Bi-Se (Bismuth-Selenium) System. *J. Phase Equil.*, 15, 195-201.
- Orujlu, E.N. (2020). Phase relations and characterization of solid solutions in the SnSb<sub>2</sub>Te<sub>4</sub>-MnSb<sub>2</sub>Te<sub>4</sub> system. *New Materials, Compounds and Applications*, 4(1), 38-43
- Pesin, D., MacDonald, A.H. (2012). Spintronics and pseudospintronics in graphene and topological insulators. *Nature Mater.*, 11, 409-416.
- Politano, A., Silkin, V.M., Nechaev, I.A., Vitello, M.S., Viti, L., Aliev, Z.S., Babanly, M.B., Chiarello, G., Echenique, P.M., Chulkov, E.V. (2015). Interplay of surface and Dirac plasmons in topological insulators: the case of Bi<sub>2</sub>Se<sub>3</sub>. *Phys. Rev. Lett.*, 115, 216802(5).
- Rowe, D.M. (2006). *Thermoelectrics Handbook: Macro to Nano*. CRC Press, Taylor & Francis Group: Boca Raton, FL, USA, 1008.
- Sher, A.A., Odin, I.E., Novoselova, A.V. (1986). Investigation of the Phases in the Bi-Se System. *Russ. J. Inorg. Chem.*, 31, 435-437.
- Shevelkov, A.V. (2008). Chemical aspects of the design of thermoelectric materials. *Russ. Chem. Rev.*, 77(1), 1-19.
- Sultana, R., Neha, P., Goyal, R., Patnaik, S.P., Awana, V.P.S. (2017). Unusual non saturating Giant Magneto-resistance in single crystalline Bi<sub>2</sub>Te<sub>3</sub> topological insulator. *J. Magn. Magn. Mater.*, 428, 213-218.
- Tumelero, M.A., Martins, M.B., Souza, P.B., Della Pace, R.D., Pasa, A.A. (2019). Effect of electrolyte on the growth of thermoelectric Bi<sub>2</sub>Se<sub>3</sub> thin films. *Electrochim. Acta*, 300, 357-362.
- Witting, I.T., Ricci, F., Chasapis, T.C., Hautier, G., Snyder, G.J. (2020). The Thermoelectric Properties of *n*-Type Bismuth Telluride: Bismuth Selenide Alloys Bi<sub>2</sub>Te<sub>3-x</sub>Se<sub>x</sub>. *Research (Washington, D.C.)*, 2020, 4361703.
- Zeynalova, G.S., Aghazade, A.I., Mirzayeva, R.C., Yusibov, Y.A., Babanli, M.B. (2021). Liquid surface of Bi<sub>2</sub> - Bi<sub>2</sub>Se<sub>3</sub> - Bi<sub>2</sub>Te<sub>3</sub> system. In Actual Problems of Modern Nat. & Econ. Sci., Ganja, 25-27.